Global NEST Journal, Vol 26, No 2, 05560

Evaluation of aqueous phase adsorption of Acid Brown on mesoporous activated carbon prepared from Azolla Pinnate seaweed

Hariharan T[1]*, Gopi Raghunadh P V S[2], Sivaramakrishnan S[3]. and Lakshmana Phaneendra Maguluri[4]
[1]Department of Chemical Engineering, Mohamed Sathak Engineering College, Kilakarai – 623806, Tamil Nadu, India.
[2]Department of Civil Engineering, Vallurupalli Nageswararao Vignana Jyothi Institute of Engineering and Technology, Hyderabad - 500090, Telangana, India
[3]Department of Civil Engineering Sri Sairam Engineering College, Chennai - 602109, Tamilnadu, India
[4]Department of Computer Science and Engineering, Koneru Lakshmaiah Education Foundation, Vaddeswaram - 522302, Andhra Pradesh, India.
Received: 20/11/2023, Accepted: 08/01/2024, Available online: 17/01/2024
*to whom all correspondence should be addressed: e-mail: hariharanthangappan@gmail.com
https://doi.org/10.30955/gnj.005560

Graphical abstract

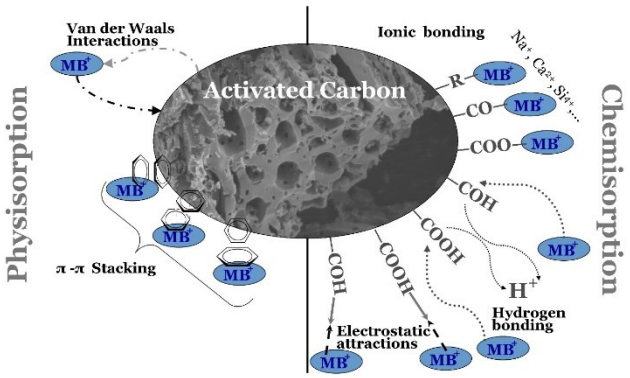

Abstract

A mesoporous activated carbon was produced from the Azolla Pinnate (AP) seaweed by two-step chemical activation technique using sulphuric acid as activating agent. The adsorption of Acid Brown (AB) from aqueous solutions is examined using the produced carbon (AP). The produced activated carbon renders a homogeneous porous structure, predominantly mesoporous with 686.5 m^2/g of BET surface area. The infra-red spectrum revealed AB affinity by multiple functional groups. The point of zero charge and the pH studies evidenced that the surface charge responsible for electronic affinity favours adsorption at higher pH. The SEM and FTIR analysis of AP before and after adsorption of acid brown shows multiple interactions, which is further substantiated by equilibrium, kinetic and thermodynamic models. Equilibrium adsorption data matched best with Langmuir isotherm model, thus primarily follows chemical interaction. However, physical affinity and heterogeneity of surface and species interaction also do exist nearly equally. Pseudo-second order kinetics provided the best explanation of the adsorption kinetics. The temperature variation studies revealed that acid brown adsorption is endothermic with high surface affinity.

Keywords: Acid Brown, azolla pinnate, activated carbon, adsorption isotherms, kinetics

1. Introduction

Synthesis of activated carbons from biomass waste is gathering pace for the last 50 years, which led to the production of activated carbons with high surface area (2000-3500 m^2/gm), unique functionalities and complex affinities from low-cost precursors. Biomass carbons have successfully replaced coal-based carbons and ease of solid waste handling. The excessive discharge of colored effluent to water bodies poses a major threat to ecosystem and public health (Robinson et al., 2001; Kheira et al., 2016). The cationic methylene blue was used frequently for dyeing wood, paper, cotton, wool and silk (Robati et al., 2016). The dye molecules released in water absorbs sun light, thereby affects the growth and existence of phytoplankton, which inturn recalcitrate the whole aquatic ecosystem. Acid Brown (AB) inhalation cause allergic rapid breathing, ingestion is also toxic to humans it may cause irritation, vomiting, diarrhea, gastric discomfort and nausea (Jie et al., 2016; Hatice & Ismet 2016; Hariharan et al., 2016). Higher doses of AB may cause methaemoglobinaemia, micturition, chest pain, stomach pain, excessive perspiration, and mental disorientation (Ahmed et al., 2009; Dimitris et al., 2015; Mehrorang et al., 2015). The major difficulty in the removal of such dyes lies in their stability and complex aromatic structure (Garg et al., 2004).

Activated carbon adsorption is widely considered as an effective process in the removal of such complex dyes for its surface electronic properties and large interior surface area. Carbon characteristics, pore structure and surface

chemistry determine its performance in adsorbing dyes. The type of precursor, the activation technique, and the degree of activation in turn affect the porous structure (Yupeng et al., 2002; Tengyan et al., 2004; Montanher et al., 2005; Chan et al., 2005). Activated carbons produced by chemical activation are mostly mesoporous (Harry & Francisco 2006), however all the three ranges of pores do exist (Rodriguez et al., 1995; Hariharan et al., 2023; Hariharan et al., 2023). The interior surface is accessible and the adsorption rate is enhanced due to a well-developed pore structure and a suitable pore size distribution (Laine et al., 1989). The surface functional group of activated carbon is the next most important factor that influences the adsorption of complex aromatic dye molecules. The surface groups containing oxygen and hydrogen strongly affects the adsorption, these surface groups may be inherited from raw material or obtained by activation (Bhabendra & Sandle 1999; Paul et al., 2003). Different groups of oxygen, including carboxyls, phenols, lactones, aldehydes, ketones, quinines, hydroquinones, anhydrides, and ether functionalities, may be present on a surface (Roop & Meenakshi 2005). Essentially in recent decades, it was established that chemical activation by two-step process resulted in adsorbent with superior qualities (Gyu & Chong 2002).

Sulphuric acid was used as activating agent for its powerful dehydrating and strong oxidizing property. It reacts with the lignocellulosic precursor by removing water and decomposing it to elemental carbon (Albert & Geoffrey 1972). Such dehydration reactions promote the partial degradation of the cellulose and hemicellulose fractions, and also contribute to structural modification of the lignin present (Caballero et al., 1997; Estefania et al., 2001; Alvarez et al., 2008; Olivares et al., 2011). H_2SO_4 improves the pore development in the carbon structure (Olivares et al., 2011); it also produces a combination of micro and meso porous carbon which is suitable for the movement of the larger AB ions. The use of H_2SO_4 for carbonization might be advantageous in terms of process cost and chemical composition of carbon produced; also, it may result in activated carbons with unique porous structures (Albert & Geoffrey 1972; Olivares et al., 2011). A two-step chemical activation using sulphuric acid was carried out on the *Areca triandra* palm husk in this study, its surface properties and AB adsorption capabilities were examined. The main focus of this study is the adsorption of AB ions from aqueous solution on activated carbon made from the Azolla Pinnate (AP) seaweed. Investigations were done on the activated carbon's ability to adsorb AB, as well as its isotherms, kinetics, mechanism, and favorability.

2. Materials and methods

2.1. Materials:

Azolla Pinnata (AP) collected from various locations in and around Nagapattinam seashore undergoes a sun-drying process for 24 hours. Subsequently, the dried material is cut into small pieces and continuously ground. In a sealed vessel, 10g each AP, along with 10mg of citric acid as a carbonization catalyst, undergo hydrothermal carbonization for five hours at a maximum temperature of 225 degrees Celsius. The resulting AP biochar is thoroughly washed with double-distilled water and dehydrated in an oven set at 176°F for half a day. To enhance the surface area of the hydro charcoal adsorbent, a hydrogen peroxide (H_2O_2) solution is utilized. The prepared hydro charcoal powder is immersed in the H_2O_2 solution for 24 hours, followed by additional heating in an oven. The sample is then collected, washed multiple times with distilled water, and prepared for further experimental procedures.

2.2. Adsorbent Preparation:

The cleaned precursor is carbonized at 350°C for three hours in a muffle furnace before being cooled to room temperature. To this pre-carbonized material conc. H_2SO_4 is added in the ratio (1:3) and allowed to react for 24 h at NTP conditions. The mixture is then brought to room temperature in a desiccator after being heated at 750°C for four hours in a muffle furnace. The products of activations were washed repeatedly with hot double distilled water followed by normal double distilled water in order to remove activation residues, until a clear supernatant with constant pH is obtained. The product, activated carbon (AP), was dried in a hot air oven, ground to the proper size, the size was separated in sieves, and the material was stored in airtight containers for additional analysis and adsorption tests. On the prepared samples, Boehm titrations and point of zero charge investigations were performed (Estefania et al., 2001).

2.3. Batch Adsorption Studies:

A set of 250 mL stoppered Erlenmeyer flasks were used for batch adsorption experiments. 10 mg of AP and 100 ml of AB solutions with varying concentrations (50-250 mg/L) were added to each flask, stirred, and stopped. Then, it is secured in an orbital shaker and shaken at 150 rpm. In a UV-Vis spectrophotometer, samples were gathered at regular intervals until they reached equilibrium and were then tested for absorbance at a wavelength of 665 nm. AP with an average particle size of 0.137 mm was used for all batch adsorption experiments (100-120 mesh). Based on the known effluent volume (L), adsorbent mass (g), initial concentration C0 (mg/L), and equilibrium concentration Ce (mg/L) of each run, the percentage of AB removal (removal %) and the adsorption capacity (qe - mg/g) for each concentration of AB at equilibrium were computed. Isotherm and kinetics models were used to analyse the findings of the adsorption studies.

2.4. Thermodynamic Studies:

The adsorption process' spontaneity, kind of reaction, and randomness are revealed by the thermodynamic parameters. The influence of temperature on the change in Gibb's free energy (G°) suggests that adsorption is feasible and spontaneous (Alvarez et al., 2008; Caballero et al., 1997; Alok 2006). The process's energy and entropy also draw attention to the adhesion mechanism. From b (L/mol), the Langmuir isotherm constant, R (J/mol K), the universal gas constant, and T (K), the absolute temperature, the free energy change G° Eqn. (1) can be calculated.

$$\Delta G^\circ = -RT\ln b \quad (1)$$

The adsorption enthalpy change (H°, J/mol) and entropy (S°, J/mol K) were calculated. using Eqn. (2):

$$\ln b = \Delta S^\circ/R - \Delta H^\circ/RT \quad (2)$$

By conducting batch adsorption investigations in an isothermal shaker at various temperatures (303, 313 & 323), the thermodynamic characteristics of adsorption were assessed.

3. Results and discussion

3.1. Surface Morphology of AP:

The surface morphology and textural properties of AP before and after adsorption of AB were determined using scanning electron microscopy (Hitachi SU-6600 Japan). The SEM image of AP (Figure 1a) shows that the activated carbon is highly porous in nature with combination of mesopores, micropores and macropores. A honey comb structure had developed during the activation of the precursor with sulphuric acid. The pores created might have undergone pore widening and transformed into wide slit shaped macropores. The geometry and distribution of the pores are determined by the characteristics of the precursor, the activating agent and the method of activation. Figure 1b shows the SEM image of AP after adsorption of AB where the surface is more irregular with non-uniform deposition. The adsorption of AB includes the interaction at the surface-active site and diffusion into the pores.

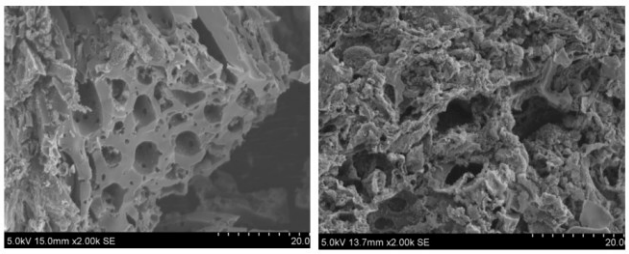

Figure 1. SEM images of AP (a) Before AB uptake and (b) After AB uptake

3.2. BET Surface Analysis of AP:

Using N_2 adsorption at 77°C, BET (NOVA, Quantachrome) analysis is used to evaluate the pore structure and specific surface area of materials. The accessible adsorption sites and a substance's sorption potential are directly related by the specific surface area. The BET isotherm of AP (Figure 2a), initially show a long shoot up at low P/P_0 followed by a long knee and a plateau, with concave shape, which represent a Type I adsorption isotherm (Sing et al., 1985). The hysteresis loop of AP shows close proximity with Type D, which characterizes the existence of slit shape pores in the microporous region (Christopher et al., 1989). Pore size distribution of the AP is shown in Figure 2c, the initial medium sized peak indicates the presence of micropores followed by the larger peak points mesopores. The linearized BET isotherm in Figure 2b indicates that AP has considerably high surface area, the plot yields the following values for the AP's BET surface area, average pore volume, and pore diameter: 686.5 m2/g, 0.2957 cc/g, and 33.91, respectively.

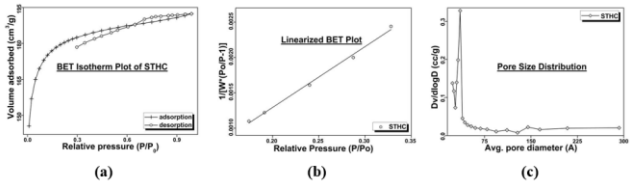

Figure 2. BET isotherm study of AP biosorbent

3.3. Surface Chemical Characteristics:

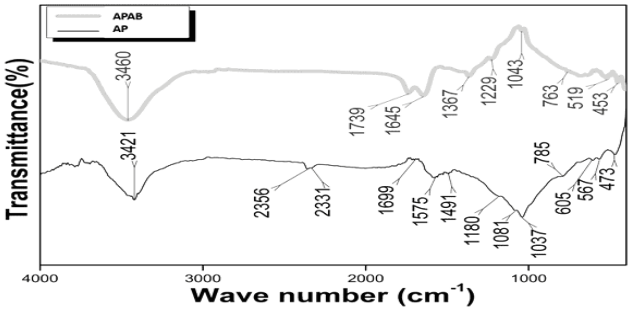

Figure 3. FTIR analysis of AP biosorbent

FTIR spectra (JASCO 6300) and CHNS (Vario EL III) analysis of AP showed characteristics of lignocellulosic biomass. The FTIR spectra of sulphuric acid activated carbon before adsorption and after AB adsorption are shown in Figure 3. Specific surface functional groups involved in interactions could be stretching vibrations of CH_2 (2356 & 2331 cm^{-1}), double bond stretching C=O of ketones (1715 cm^{-1}), C=O stretching of carboxylic acid dimers (1699 cm^{-1}), N=O of organic nitro and N-nitroso compounds (1575 &1491 cm^{-1}), C-O of alcohols stretching (1180 & 1081 cm^{-1}), C-O of primary alcohols (1037 cm^{-1}) and aromatic CH wagging (785 & 763 cm^{-1}). The shifting of peaks shows that there was AB binding process occurring in the surface of the carbon. Remarkable difference in the absorption spectrum is noticed in the region between 1450 and 700 cm^{-1}.

The columbic interaction between the adsorbent surface and the adsorbate in the liquid phase is shown by the point of zero charge (pH_{PZC}). As demonstrated in Figure 4, the pH of the final solution rises as adsorbent is present until it reaches the inversion point known as pH_{PZC}. The following Eqn. can be used to describe the electrical charge at the adsorbent surface to protonating or deprotonating (3, 4) and at the point of zero charge in Eqn. (5);

$$\text{-MOH} + \text{H+} \rightarrow \text{MOH2+} \quad (3)$$

$$\text{-MOH} + \text{OH-} \rightarrow \text{-MO-} + \text{H2O} \quad (4)$$

$$[\text{MOH2+}] \leftrightarrow \text{-MO-} + \text{H2O} \quad (5)$$

At lower pH the surface of the activated carbons is protonated and acidic with positive charges. This electrostatic repulsion between AB cations and the AP surface do not support the adsorption. At higher pH the surface acquires negative charges resulting in electrostatic attraction. The Boehm titration values and FTIR support

this observation, increased basicity of the surface by sulphuric acid activation and the increased capacity at higher pH. The fact that the point of zero charge (pH_{PZC}) for AP is 9.3 pH reveals that the surface is basic in nature and the degree of surface oxidation (Ania et al., 2002), above 9.3 pH, the surface develops a net negative charge; higher solution pH promotes AB adsorption. Table 1 displays the results of the AP Boehm titrations (Naiqin et al., 2005). The precursor has more acidic groups than basic groups, whereas AP have more basic groups than acidic groups reinforcing the higher pH_{PZC}, phenolic groups are predominant among acid groups.

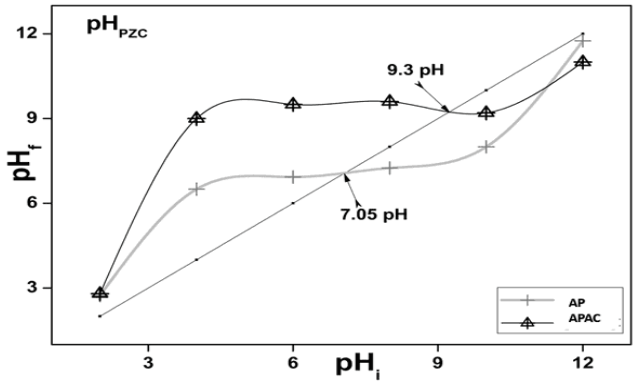

Figure 4. pH_{ZPC} of the biosorption of AB using AP

Table 1. Boehm titrations results

Material	Basic (mmol/g)	Carboxylic (mmol/g)	Lactonic (mmol/g)	Phenolic (mmol/g)	pH_{pzc} pH
RAW AP	0.22	0.12	0.17	0.19	7
Activated AP	0.56	0.11	0.12	0.196	9.3

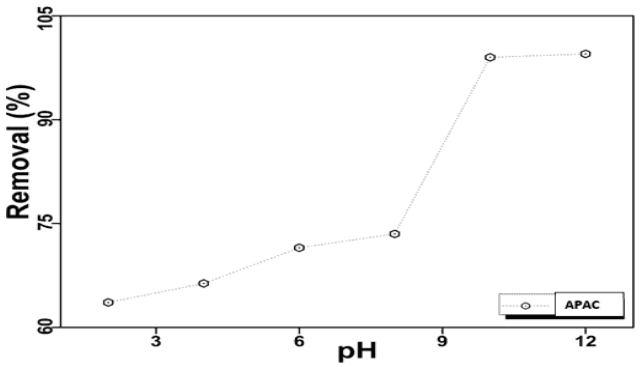

Figure 5. Impact of pH by in AB adsorption

The way that a dye molecule adheres to the adsorbent surface is significantly influenced by pH. The degree of AB ionisation and the dissociation of functional groups on the carbon surface are both influenced by the pH. As demonstrated in Figure 5, the AB adsorption rises gradually at lower pH values and sharply from pH 8 to 10. The electrostatic interaction between the AP surface and the AB molecules increased at higher pH levels.

3.4. Equilibrium Adsorption Data Analysis:

Adsorption system analysis and design heavily rely on adsorption isotherm models. Three models connect the solute concentrations in solutions at equilibrium at a particular temperature to the amount of solute adsorbed on the unit mass of adsorbent. For the examination of adsorption data, some of the most used models include Temkin's isotherm, Freundlich isotherm, and Langmuir isotherm. The way the adsorbate dye molecule interacts with the adsorbent surface affects the adsorption mechanism. Van der Waals forces, hydrogen bonds, hydrophobic forces, and chemical bonds may all be involved in this interaction (Yennam et al., 2014).

Table 2. Isotherm model equations

Isotherm Model	Linearized form	Eqn.	Plots
Langmuir	$C_e/q_e = 1/K_L * q_m + C_e/q_m$	(7)	C_e/q_e versus C_e
Freundlich	$q_e = K_F C_e^{1/n}$	(8)	*ln* q_e versus *ln* C_e
Temkin	$q_e = RT/B \ln(AC_e)$	(9)	q_e versus *ln* C_e

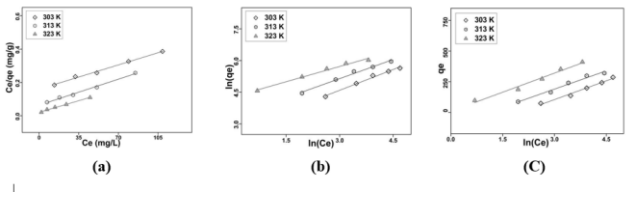

Figure 6. Isotherm studies of (a) Langmuir, (b) Freundlich and (c) Temkin models for AB adsorption using AP

The Langmuir isotherm presupposes that the adsorbate molecule interacts with the adsorbent surface with uniform active sites and that a monolayer form on the surface (Hameed 2009). A dimensionless separation factor R_L is given by the Eqn. 6, the value of the separation factor R_L indicates whether the isotherm type is unfavourable adsorption ($R_L > 1$), linear ($R_L = 1$), favorable ($0 < R_L < 1$), or irreversible ($R_L = 0$). The Freundlich model assumes that adsorption is possible in multilayer on a highly heterogeneous surface comprising of non-identical and non-uniform energy sites (Hong et al., 2009). In addition to adsorbate-adsorbent interactions, the Temkin model also takes into account binding heterogeneity and indirect adsorbate to adsorbate attractions. According to this isotherm, the heat of adsorption for every molecule in the layer will fall linearly, and the distribution of binding energies will be uniform up to a limiting binding energy (Hong et al., 2009). Table 2 gives the equations for the linearized isotherm model and the related graphs.

$$R_L = \frac{1}{1 + K_L * C_0} \quad (6)$$

Where, q_m (mg/g) are the amount of dye adsorbed per unit mass of sorbent at equilibrium concentration (for complete monolayer formation), K_L (L/mg) is the Langmuir equilibrium constant related to the affinity of binding sites and energy of adsorption. K_F (L/mmol) is the Freundlich

isotherm constant, n is the intensity of adsorption and $n > 1$ favours the adsorption process. R (J/mol°K) the universal gas constant, T (°K) the absolute temperature, B (J/mol) and A (L/g) are Temkin's constants related to heat of sorption and isotherm constant respectively.

Table 3. Isotherm model constants and coefficients

Isotherm Model	Temperature K	Parameters			R^2
Langmuir	303	q_m= 480.7	K_L = 0.013	R_L = 0.489	0.991
	313	q_m= 492.6	K_L = 0.033	R_L = 0.283	0.991
	323	q_m= 502.5	K_L = 0.095	R_L = 0.131	0.990
Freundlich	303	K_F = 13.76	n = 1.523		0.985
	313	K_F = 27.91	n = 1.656		0.983
	323	K_F = 71.81	n = 2.079		0.983
Temkin	303	A = 7.176	B = 102		0.980
	313	A = 2.991	B = 99.6		0.973
	323	A = 1.079	B = 104		0.975

The linearized isotherms in Figure 6 are shown in Table 3 together with the model's parameters. With a correlation coefficient of 0.99 for all the temperatures examined, the Langmuir isotherm provided a very good fit to the data, and as temperature rises, so does adsorption capacity. The adsorption of AB on AP is advantageous, as evidenced by the computed value of the dimensionless constant RL, which ranges from 0 to 1. It demonstrates that AB is adsorbed in a monolayer on AP. Figure 6b depicts how well the model fits the data. With the presumptions of heterogeneous surface activity and the adsorption intensity varying exponentially with adsorption heat, the linear form of the Freundlich equation is constructed. The variability of the surface activity of the AB adsorption on AP is supported by the correlation coefficient value and the Freundlich exponent n, value. The Temkin isotherm is derived under the presumption that as surface coverage increases, adsorption heat decreases. All three isotherms fit the adsorption data in the investigated concentration range, as shown in Figure 6.

3.5. Adsorption Kinetics Data Analysis:

In order to understand the mechanism of the adsorption process and to assess the experimental rate data, kinetic models are used. For the selection and design of the adsorption system, knowledge of adsorption kinetics is crucial. By comparing the batch kinetic data with the Pseudo-first order, Pseudo-second order, and intra-particle diffusion models, a suitable kinetics equation is chosen. A first order rate equation based on adsorption capacity is represented by the pseudo-first order model (Ho and Mckay 1998). According to the Pseudo-second order model, the adsorption kinetic is second-order, and the rate-limiting step is a chemical process involving valent forces through electron sharing or exchange. Assuming that, the Langmuir isotherm model governs adsorption (Ho and Mckay 1998; Ho and Mckay 1999).

The homogeneous solid diffusion model (HSDM), also known as the intra-particle diffusion model, postulates that mass transfer within an amorphous, homogeneous sphere is the limiting step. Many adsorption investigations have shown that adsorbate absorption changes with $t^{1/2}$ rather than t. In order to determine if intra-particle diffusion is the only limiting step, this model is used (Yennam et al., 2014). Table 4 displays the governing equations for each of the three kinetic models along with the corresponding graphs. Where, q_t (mg/g) is the adsorption capacity at any instant of time, k_{p1} (min^{-1}) is the pseudo-first-order rate constant for the kinetic model. K_{p2} (g/(mg.min)) is the pseudo-second order rate constant and k_{int} (min^{-1}) is the intra-particle diffusion rate constant. With the help of experimental data on the AB adsorption on AP, pseudo-first order, pseudo-second order, and intra-particle diffusion models are evaluated.

Table 4. Kinetic model equations

Kinetic Model	Linearized form	Eqn.	Plots
Pseudo-first order	$dqt/dt = k_{p1}(q_e - q_t)$	(10)	$ln\ (q_e - q_t)$ versus t
Pseudo-Second Order	$dqt/dt = k_{p2}(q_e - q_t)^2$	(11)	t/q_t versus t
Intra-particle diffusion	$q_t = k_{int} t^{1/2}$	(12)	q_t versus $t^{1/2}$

Table 5. Kinetic model constants and coefficients

Kinetic Model	Ci -ppm	Parameters		R^2
Pseudo-First order	80	k_{p1} = 0.0507	q_e = 9.253	0.905
	60	k_{p1} = 0.0713	q_e = 9.235	0.976
	40	k_{p1} = 0.0713	q_e = 8.069	0.953
Pseudo-Second order	80	k_{p2} = 0.029	q_e = 200	0.991
	60	k_{p2} = 0.031	q_e = 166.6	0.992
	40	k_{p2} = 0.043	q_e = 111.1	0.995
Intra-Particle diffusion	80	k_{int} = 8.869		0.923
	60	k_{int} = 15.25		0.971
	40	k_{int} = 12.61		0.907

Table 5 displays the model parameters and correlation coefficients. Pseudo-second order model, one of the investigated models, has a 0.99 correlation coefficient with the experimental data. The pseudo-second order model is predicated on the idea that chemisorption, which involves valence forces through the sharing or exchange of electrons between sorbent and sorbate, may be the rate-limiting phase (Ho and Mckay 1998). The outcome indicates that there are electrical interactions between the AB dye and the heterogeneous AP surface.

The first stage corresponds to the initial binding of the AB molecule with the solid surface's active spots. Since there are no other molecules present, the sorbate-sorbate interactions are minimal, which results in the formation of a monolayer. This interpretation can be made from the two linear regions in the pseudo-first order model in Figure 7a. Rearranging the sorbate molecules may take place as this monolayer approach's saturation, leading to an increase in sorbate molecules and the second linear step (Varshney et al., 1996).

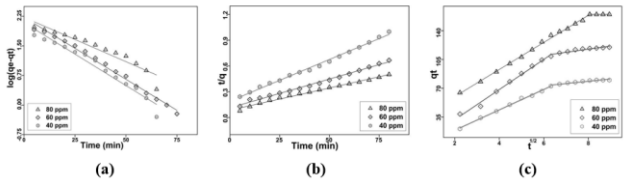

Figure 7. Adsorption kinetic studies of (a) Pseudo-first order, (b) Pseudo-second order and (c) Intra-particle diffusion models for AB adsorption using AP

Figure 7c shows the AB adsorbed (qt) against $t^{1/2}$. Two linear steps are shown in the plot, signifying two processes. The exterior surface diffusion is indicated by the first step, while the adsorption process is indicated by the second step, where intra-particle diffusion is rate limiting. There is no straight line in the qt vs $t^{1/2}$ figure. Travelling through the origin, show that, there are other rate-limiting processes besides intra-particle diffusion. Kinetics is also impacted by film diffusion (Gurusamy & Menjeri 1997).

3.6. Thermodynamic Parameters:

Table 6 lists the thermodynamic parameters for AB adsorption on AP. The values of G° were observed to decrease with rise in temperature suggests that higher temperature favors AB adsorption. The negative Gibb's free energy (G°) for three temperatures imply that adsorption is feasible and spontaneous. Adsorption is endothermic, according to the positive enthalpy change (H°) value (78.1 kJ/mol), which supports the finding that adsorption rate rises with temperature. Additionally, the increased randomness at the AP-AB interface is confirmed by the positive entropy (S°) (269.7 J/mol K), which shows that AB ions have replaced the previously adsorbed water molecules with ones that have a stronger affinity (Yasemin & Haluk 2006; Nasuha & Hameed 2011).

Table 6. Thermodynamic parameters

T (K)	ΔG° (kJ/mol)	ΔH° (kJ/mol)	ΔS° (J/mol K)
303	- 3.617	78.1	269.7
313	- 6.287		
323	- 9.012		

3.7. AB Adsorption Mechanism:

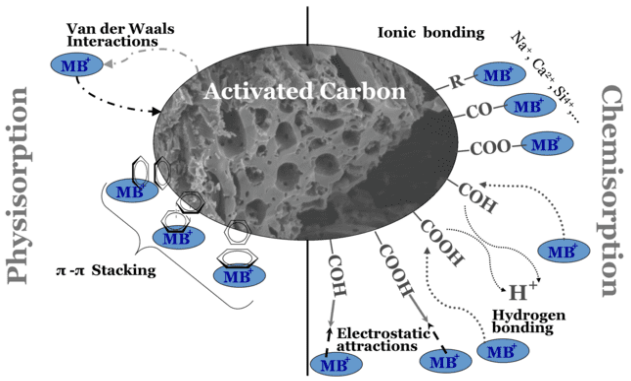

Figure 8. Adsorption mechanism of AB using AP biosorbent

The dye ions and carbon surface experiences physical and chemical interactions by nature, namely electrostatic or non-electrostatic (van der Waals forces, hydrophobic interactions and hydrogen bonding) (Shilpi et al., 2016). The adsorption of AB on the heterogeneous adsorbent AP involves physical activity i.e., the van der Waals force of attractions and electrostatic attraction and electronic/chemical bonding (Figure 8). The pH*pzc* and pH analysis indicate the electrostatic interaction between AB and AP. The FTIR analysis shows the role of surface complexation between the AB and AP. The functional groups -OH, -COOH, -CO and –CH functional groups might be participating in AB binding. The kinetic studies affirm the binding of AB on AP (Fatma et al., 2016; Shisuo et al., 2016). Below pH 9, the electrostatic attraction between the functional groups and the anionic dye molecule may be the cause of the dye molecules adhering to the adsorbent, and above pH 9.3, the carboxylic groups may be deprotonated, causing the negatively charged carboxylate ligand to bind to the positively charged AB molecule. The aromatic structures of AB make the adsorption easy by π-π stacking interactions which contribute to the shifting and weakening of the peaks (Fatma et al., 2016).

4. Conclusions

Activated carbon prepared from AP by two-step H_2SO_4 activation resulted with good adsorbent properties, moderate surface area having combination of three types of pores suitable for easy toxin transport, surface morphology showing cylindrical pores with network, well oxidized surface with basic nature and a variety of surface functionality having affinity for toxins with different charges. Higher pH values favor AB molecule adsorption. The adsorption process, which is governed by chemical reaction, is defined by pseudo-second order kinetics, according to kinetic studies. The endothermic nature of the

process is confirmed by the positive enthalpy change, the strong affinity for AB is indicated by the positive entropy, and the negative values of Gibb's free energy values support the spontaneity of the adsorption. Thus, all the studies suggest that the activated carbon prepared have good qualities of adsorbent suitable for AB dye removal.

References

A. Ahmad, M. Rafatullah, O. Sulaiman, M.H. Ibrahim. and R. Hashim. (2009). Scavenging behaviour of meranti sawdust in the removal of methylene blue from aqueous solution, Journal of Hazardous Materials, **170**, 357–365

Alok Mittal. (2006). Adsorption kinetics of removal of a toxic dye, Malachite Green, from wastewater by using hen feathers, Journal of Hazardous Materials, **133**, 196–202

Alvarez-Merino MA, Fontecha-Camara MA, Lopez-Ramon MV. and Moreno-Castilla C. (2006). Temperature dependence of the point of zero charge of oxidized and non-oxidized activated carbons, Carbon, **46**, 778–787

Ania C. O, Parra J. B. and Pis J. J. (2002). Influence of oxygen-containing functional groups on active carbon adsorption of selected organic compounds, Fuel Processing Technology, **79**, 265–271

Bhabendra K Pradhan. and NK Sandle. (1999). Effect of different oxidizing agent treatments on the surface properties of activated carbons, Carbon, **37**, 1323–1332

Caballero JA, Marcilla A. and Conesa JA. (1997). Thermogravimetric analysis of olive stones with sulphuric acid treatment, Journal of Analytical and Applied Pyrolysis, **44**, 75–88

Chan-Jun Moon. and Jung-heon Lee. (2005). Use of curdlan and activated carbon composed adsorbents for heavy metal removal, Process Biochemistry, **40**, 1279–1283

Christopher GVB, Douglas HE. and Stuart Nuttall. (1989). Adsorption hysteresis in porous materials, Pure and Applied Chemistry, **61**, 1845–1852

D Robati, S Bagheriyan, M Rajabi, O Moradi. and A Ahmadi Peyghan. (2016). Effect of electrostatic interaction on the methylene blue and methyl orange adsorption by the pristine and functionalized carbon nanotubes, Physica E, **83**, 1–6

Dimitris Mitrogiannis, Giorgos Markou, Abuzer Celekli. and Huseyin Bozkurt. (2015). Biosorption of methylene blue onto Arthrospira platensis biomass: Kinetic, equilibrium and thermodynamic studies, Journal of Environmental Chemical Engineering, **3**, 670–680

Estefania Iniesta, Francisca Sanchez, Garcia AN. and Antonio Marcilla. (2001). Yields and CO_2 reactivity of chars from almond shells obtained by a two heating step carbonization process. Effect of different chemical pre-treatments and ash content, Journal of Analytical and Applied Pyrolysis, **58**, 983–994

F Albert Cotton. and Geoffrey Wilkinson. (1972). Advanced inorganic chemistry – A comprehensive text. 3rd ed. John Wiley & Sons: Interscience Publishers.

F Rodriguez-Reinoso, M Molina-Sabio. and MT Gonzalez. (1995). The use of steam and CO_2 as activating agents in the preparation of activated carbons, Carbon, **33**, 15–23

Fatma Kallel, Fatma Chaari, Fatma Bouaziz, Fedia Bettaieb, Raoudha Ghorbel. and Semia Ellouz Chaabouni. (2016). Sorption and desorption characteristics for the removal of a toxic dye, methylene blue from aqueous solution by a low-cost agricultural by-product. Journal of Molecular Liquids, **219**, 279–288

Gurusamy Annadurai. and Menjeri RV Krishnan. (1997). Batch equilibrium adsorption of reactive dye onto natural biopolymer, Iranian Polymer Journal, **6**, 167–175

Gyu Hwan Oh. and Chong Rae Park. (2002). Preparation and characteristics of rice-straw-based porous carbons with high adsorption capacity, Fuel, **81**, 327–336

Hameed BH. (2009). Evaluation of papaya seeds as a novel non-conventional low-cost adsorbent for removal of methylene blue, Journal of Hazardous Materials, **162**, 939–944

Hariharan T, Gokulan R, Al-Zaqri N. and Warad I. (2023). Enhanced biosorption of hexavalent chromium ions from aqueous solution onto Ziziphus jujube seeds as ecofriendly biosorbent – equilibrium and kinetic studies, Desalination and Water Treatment, **295**, 205–216

Hariharan T, Gokulan R, Venkat Saravanan R. and Zunaithur Rahman D. (2023). Batch and packed bed column studies of azo dyes adsorption from the aqueous solutions using activated sugarcane bagasse charcoal adsorbent: isotherm and kinetic studies, Global NEST Journal, **25(1)**, 151–168

Hariharan Thangappan, Arjun VP. and Shiny Joseph. (2016). Surface characterization and methylene blue adsorption studies on a mesoporous adsorbent from chemically modified *Areca triandra* palm shell, Desalination Water Treat, **57**, 21118–21129

Harry Marsh. and Francisco Rodriguez-Reinoso. (2006). Activated Carbon. 1st ed. Elsevier Science & Technology Books.

Hatice Karaer. and Ismet Kaya. (2016). Synthesis, characterization of magnetic chitosan/active charcoal composite and using at the adsorption of methylene blue and reactive blue, Microporous and Mesoporous Materials, **232**, 26–38

Ho YS. and Mckay G. (1998). A comparison of chemisorption kinetic models applied to pollutant removal on various sorbents, Transactions of the Institution of Chemical Engineers, **76B**, 332–340

Ho YS. and Mckay G. (1998). Kinetic models for the sorption of dye from aqueous solution by wood, Transactions of the Institution of Chemical Engineers, **76B**, 183–191

Ho YS. and McKay G. (1999). Pseudo-second order model for sorption processes, Process Biochemistry, **34**, 451–465

Hong Zheng, Donghong Liu, Yan Zheng, Shuping Liang. and Zhe Liu. (2009). Sorption isotherm and kinetic modeling of aniline on Cr–bentonite, Journal of Hazardous Materials, **167**, 141–147

J Laine, A Calafat. and M Labady. (1989). Preparation and characterization of activated carbons from coconut shell impregnated with phosphoric acid, Carbon, **27**, 191–195

J Paul Chen, Shunnian Wu. and Kai-Hau Chong. (2003). Surface modification of a granular activated carbon by citric acid for enhancement of copper adsorption, Carbon, **41**, 1979–1986

Jie Chen, Jiangtao Feng. and Wei Yan. (2016). Influence of metal oxides on the adsorption characteristics of PPy/metal oxides for Methylene Blue, Journal of Colloid and Interface Science, **475**, 26–35

KG Varshney, AA Khan, U Gupta. and SM Maheshwari. (1996). Kinetics of adsorption of phosphamidon on antimony (V) phosphate cation exchanger: evaluation of the order of reaction and some physical parameters, Colloids and

Surfaces, A: Physicochemical and Engineering Aspects, **113**, 19–23

Kheira Chinoune, Kahina Bentaleb, Zohra Bouberka, Abdelouahab Nadim. and Ulrich Maschke. (2016). Adsorption of reactive dyes from aqueous solution by dirty bentonite, Applied Clay Science, **123**, 64–75

Mehrorang Ghaedi. and Syamak Nasiri Kokhdan. (2015). Removal of methylene blue from aqueous solution by wood millet carbon optimization using response surface methodology, Spectrochimica Acta, Part A: Molecular and Biomolecular Spectroscopy, **136**, 141–148

Naiqin Zhao, Na Wei, Jiajun Li, Zhijun Qiao, Jing Cui. and Fei He. (2005). Surface properties of chemically modified activated carbons for adsorption rate of Cr (VI), Chemical Engineering Journal, **115**, 133–138

Nasuha N. and Hameed BH. (2011). Adsorption of methylene blue from aqueous solution onto NaOH-modified rejected tea, Chemical Engineering Journal, **166**, 783–786

Olivares-Marin M, Fernandez-Gonzalez C, Macias-Garcia A. and Gomez-Serrano V. (2011). Preparation of activated carbon from cherry stones by physical activation in air - Influence of the chemical carbonization with H_2SO_4, Journal of Analytical and Applied Pyrolysis, **94**, 131–137

Roop Chand Bansal. and Meenakshi Goel. (2005). Activated carbon adsorption, 1st ed. CRC Press: Taylor & Francis Group.

SF Montanher, EA Oliveira. and MC Rollemberg. (2005). Removal of metal ions from aqueous solutions by sorption onto rice bran, Journal of Hazardous Materials, **117B**, 207–211

Shilpi Agarwal, Inderjeet Tyagi, Vinod Kumar Gupta, Nahid Ghasemi, Mahdi Shahivand. and Maryam Ghasemi. (2016). Kinetics, equilibrium studies and thermodynamics of methylene blue adsorption on Ephedra strobilacea saw dust and modified using phosphoric acid and zinc chloride, Journal of Molecular Liquids, **218**, 208–218

Shisuo Fan, Jie Tang, Yi Wang, Hui Li, Hao Zhang, Jun Tang, ZhenWang. (2016). Xuede Li, Biochar prepared from co-pyrolysis of municipal sewage sludge and tea waste for the adsorption of methylene blue from aqueous solutions: Kinetics, isotherm, thermodynamic and mechanism, Journal of Molecular Liquids, **220**, 432–441

Sing KSW, Everett DH, Haul RAW, Moscou L, Pierotti RA, Rouquerol J. and Siemieniewska T. (1985). Reporting physisorption data for Gas/Solid systems with special reference to the determination of surface area and porosity, Pure and Applied Chemistry, **57**, 603–619

T Robinson, G McMullan, R Marchant. and P Nigam. (2001). Remediation of dyes in textile effluent. A critical review on current treatment technologies with a proposed alternative, Bioresource Technol, **77**, 247–255.

Tengyan Zhang, Walawender PW, Fan LT, Maohong Fan, Daren Daugaard. and Brown RC. (2004). Preparation of activated carbon from forest and agricultural residues through CO_2 activation, Chemical Engineering Journal, **105**, 53–59

VK Garg, Moirangthem Amita, Rakesh Kumar. and Renuka Gupta. (2004). Basic dye (methylene blue) removal from simulated wastewater by adsorption using Indian Rosewood sawdust: a timber industry waste, Dyes Pigments, **63**, 243–250

Yasemin Bulut. and Haluk Aydin. (2006). A kinetics and thermodynamics study of methylene blue adsorption on wheat shells, Desalination, **194**, 259–267

Yennam Rajesh. and Murali Pujari, R. (2014). Uppaluri, Equilibrium and kinetic studies of Ni (II) adsorption using pineapple and bamboo stem based adsorbents, Separation Science and Technology, **49**, 533–544

Yupeng Guo, Jurui Qi, Shaofeng Yang, Kaifeng Yu, Zichen Wang. and Hongding Xu. (2002). Adsorption of Cr(VI) on micro- and mesoporous rice husk-based active carbon. Materials Chemistry and Physics, **78**, 132–137